

⁴L. R. Elton and A. Swift, Nucl. Phys. **A94**, 52 (1967); C. J. Batty and G. W. Greenless, Nucl. Phys. **A133**, 673 (1969).

⁵J. W. Negele, Phys. Rev. C **1**, 1260 (1970); D. Vautherin and D. M. Brink, Phys. Lett. **32B**, 149 (1970); H. C. Lee and R. Y. Cusson, Nucl. Phys. **A170**, 439 (1971); R. J. Lombard, Phys. Lett. **32B**, 652 (1970); R. C. Barrett, Rep. Prog. Phys. **37**, 1 (1974), and J. Phys. (Paris), Colloq. **C4**, 23 (1973).

⁶F. Binon, P. Duteil, J.-P. Garron, J. Gorres, L. Hugon, J.-P. Peigneux, C. Schmit, M. Spighele, and J.-P. Stroot, Nucl. Phys. **B17**, 168 (1970).

⁷J. Ashkin, J.-P. Blaser, F. Feiner, and M. O. Stern,

Phys. Rev. **101**, 1149 (1956); P. J. Bussey, J. R. Carter, D. R. Dance, D. V. Bugg, A. A. Carter, and A. M. Smith, Nucl. Phys. **B58**, 363 (1973).

⁸J.-F. Germond and C. Wilkin, Nucl. Phys. **A249**, 457 (1975).

⁹Hans A. Bethe and Mikkel B. Johnson, LASL Report No. LA-UR-76-1844, 1976 (unpublished), and private communication.

¹⁰M. J. Jakobson, G. R. Burleson, J. R. Calarco, M. D. Cooper, D. C. Hagerman, I. Halpern, R. H. Jeppeson, K. F. Johnson, L. D. Knutson, R. E. Marrs, H. O. Meyer, and R. P. Redwine, Phys. Rev. Lett. **38**, 1201 (1977).

Analysis of the Lamp-Dip Structure with Linear and Helicoidal Polarizations

A. Le Floch

Laboratoire d'Electronique Quantique, Université de Rennes, 35031 Rennes Cedex, France

and

R. Le Naour

Laboratoire d'Electronique Quantique, Université de Nantes, 44037 Nantes Cedex, France

and

G. Stephan

Institut de Physique, Université d'Oran, Oran, Algérie

(Received 23 March 1977; revised manuscript received 25 October 1977)

A simple differential analysis of the Lamb-dip structure using a stationary helicoidal wave is described. This technique enables us to separate the anisotropic contribution from the isotropic one and shows that the observed Lamb dip on the $3.39\text{-}\mu\text{m}$ line of Ne²⁰ is partially anisotropic.

The Lamb dip predicted by Lamb's self-consistency theory¹ has been studied by many authors, both experimentally² and theoretically.³ The usual observation is performed on the output power of a linearly polarized monomode laser. This resonance at the center of a Doppler profile is described in the scalar theory as a Lorentzian of width $2\gamma_{ab}$. The "hole-burning" concept introduced by Bennett⁴ gives a simple phenomenological interpretation of the resonance by merging at line center of two atomic packets which interact with the two progressive waves of the stationary mode. In a recent probe experiment⁵ on the active column of an He-Ne laser, we have directly shown and measured the induced anisotropies occurring in the "atoms+field" system. That is to say, we have isolated the anisotropic contribution of the saturation depending on the level degeneracies which were previously considered in Zee-man laser theory.⁶ We describe a new experiment using a stationary helicoidal wave on the $3.39\text{-}\mu\text{m}$ line of Ne²⁰ which allows the study of the Lamb-

dip structure by observation of its isotropic and anisotropic parts. This simple differential analysis shows that, on this particular line, the Lamb dip is partially anisotropic and necessitates an interpretation in the spatial vectorial model,⁷ even in zero magnetic field. According to Bennett's physical interpretation of the Lamb dip, it is then necessary to introduce the concept of "aligned holes."

The scheme of the apparatus is shown in Fig. 1(a). A monomode laser with a stationary field having either a linear or a helicoidal structure is realized. When both slow axes of the $\lambda/4$ plates are in the incidence plane of the Brewster window, the polarization of the field is linear [Fig. 1(b)] all along the laser. On the contrary, if the $\lambda/4$ plate No. 1 is rotated through $\pm 45^\circ$, the stationary field in the active medium between the two plates is represented by either a right-handed or a left-handed helix [Fig. 1(c)]; this field configuration has been proposed by Evtuhov and Siegman⁸ and by Kastler,⁹ and has been experimental-

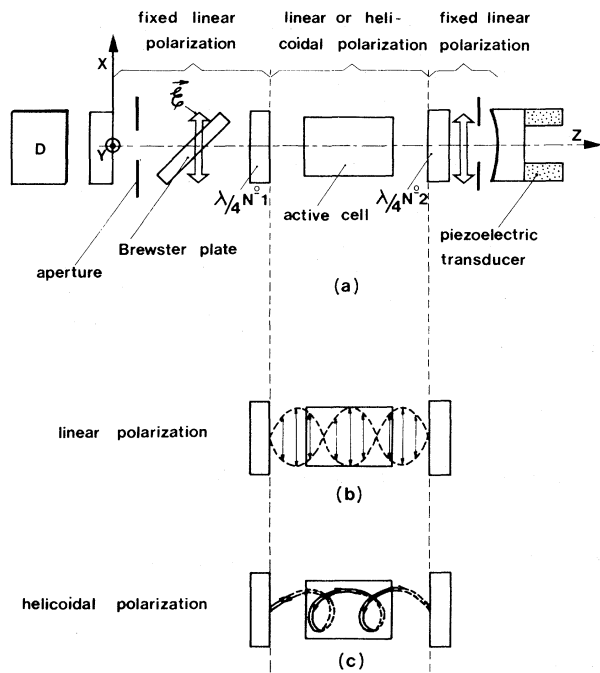


FIG. 1. Schematic of the experimental apparatus.

ly analyzed on the $\lambda = 3.39 \mu\text{m}$ line.¹⁰ Our experiment enables one to compare, without varying any other parameter, the Lamb-dip shape in both cases. We notice that indeed the laser field is the same beyond the two $\lambda/4$ plates, and so the losses are left unchanged. When the field is helicoidal, the two counterpropagating waves are both circularly polarized, one right-handed σ^+ and another left-handed σ^- . Note that the stationary

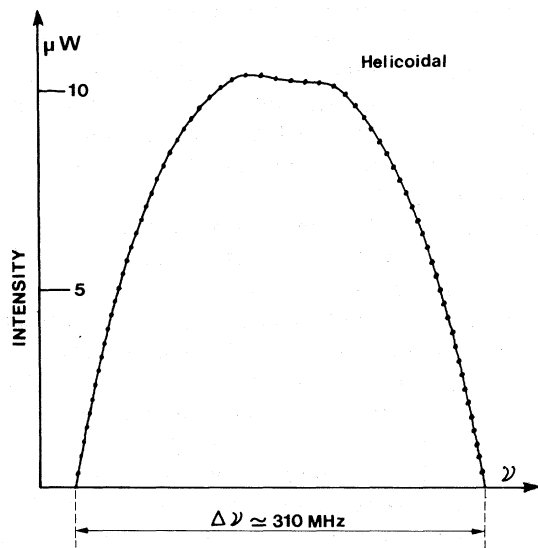


FIG. 3. Theoretical curve and experimental points of the output intensity with a stationary helicoidal field.

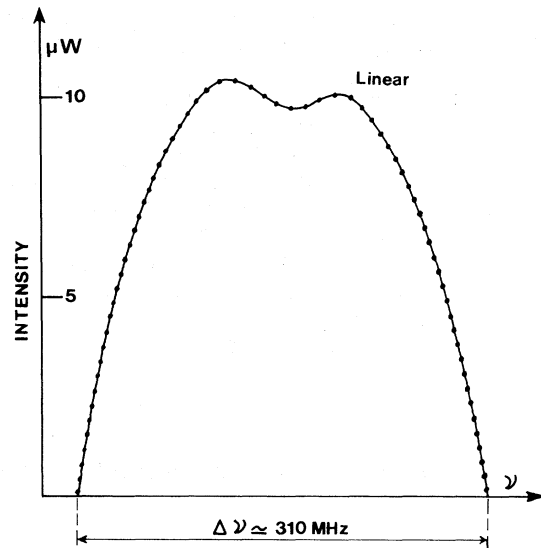


FIG. 2. Theoretical curve and experimental points of the output intensity with a linearly polarized field.

helicoidal wave has a constant amplitude and must be distinguished from a circular stationary wave. On the contrary, when the field is linearly polarized, each progressive wave contains both σ 's and so creates alignment. The saturation has then, in this case, two physical origins¹¹: a scalar one due to level populations and a tensorial one due to alignment (or Zeeman coherences). In the case of the stationary helicoidal wave, each progressive wave creates orientation instead of alignment and so the second type of saturation must disappear, and the total saturation at the line center decreases. The experimental results reported on Figs. 2 and 3 confirm this structure. With the experimental conditions (total pressure

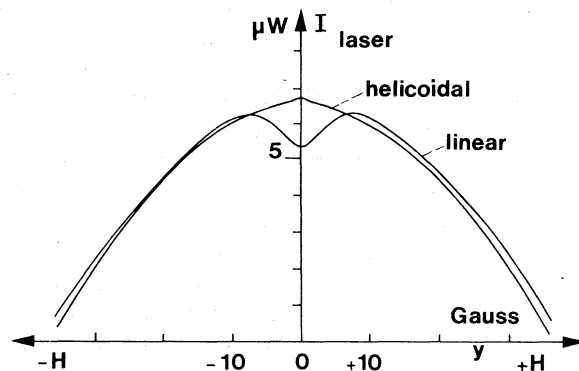


FIG. 4. Zero-field magnetic resonances for the two polarized fields.

0.6 Torr, ratio $\text{Ne}^{20}/\text{He}^3 \approx \frac{1}{7}$, output power ≈ 10 μW , the Lamb dip on the 3.39- μm line with linear polarization is partially due to the alignment of the 3P_4 level, that is, due to the anisotropic contribution. This can be confirmed by studying the magnetic resonance at zero field, when an axial magnetic field is applied to the active medium. Figure 4 shows that the zero-field resonance (due essentially to Zeeman coherences) for a fixed mode position out of the line center disappears completely in the case of the helicoidal wave.

A previous analysis¹¹ of the anisotropies induced by the saturating field in the active column of the laser enables us to calculate by application of the resonance condition⁷ the expression of the output power, for both linearly polarized and helicoidal waves. The resonance condition is written

as

$$\mathcal{P}_2 \mathcal{R}_2 \mathcal{P}_1 \mathcal{R}_1 \vec{\mathcal{E}} = \vec{\mathcal{E}}, \quad (1)$$

where

$$\mathcal{R}_1 = \begin{pmatrix} r_x & 0 \\ 0 & r_y \end{pmatrix}, \quad \mathcal{R}_2 = r \begin{pmatrix} 1 & 0 \\ 0 & 1 \end{pmatrix}$$

are the Jones reflection matrices. $\mathcal{P}_{1,2}$ represent the propagation matrices calculated in reference¹¹ for each propagating wave. In the case of linear polarization, for a laser of length L ,

$$\mathcal{P}_{1,2} = \begin{pmatrix} e^{ik_x L} & 0 \\ 0 & e^{ik_y L} \end{pmatrix},$$

so that the resonance condition for the x lasing component may be written as

$$k_x = (2iL)^{-1} \ln(rr_x)^{-1}. \quad (2)$$

In the case of the linearly polarized field with k_x calculated up to third order by the usual perturbation theory, this leads to

$$I_l = \mathcal{E}_l^2 = \left[\frac{1}{L} \ln \frac{1}{rr_x} - \frac{2\omega N_0 S}{\epsilon_0 c \hbar k v_m} Z^i(\xi) \right] \left\{ \frac{2\omega N_0}{\epsilon_0 c \hbar} \left[\text{Re}(I_1 + I_2) \right] \left(\frac{S_1 + S_3}{\Gamma_a'(0)} + \frac{S_1 + S_2}{\Gamma_a'(0)} + \frac{S_2}{\Gamma_b'(2)} + \frac{S_3}{\Gamma_b'(2)} \right) \right\}^{-1}. \quad (3)$$

In the case of an helicoidal polarized field, the losses remain unchanged and (2) leads to the intensity

$$I_h = \mathcal{E}_h^2 = \left[\frac{1}{L} \ln \frac{1}{rr_x} - \frac{2\omega N_0 S}{\epsilon_0 c \hbar k v_m} Z^i(\xi) \right] \left\{ \frac{2\omega N_0}{\epsilon_0 c \hbar} \left[2 \text{Re} I_1 \left(\frac{S_1}{\Gamma_a'(0)} + \frac{S_1}{\Gamma_b'(0)} \right) + 2 \text{Re} I_2 \left(\frac{S_2}{\Gamma_b'(0)} + \frac{S_3}{\Gamma_a'(0)} \right) \right] \right\}^{-1}. \quad (4)$$

If we let d_l and d_h denote, respectively, the denominators of expressions (3) and (4), the above intensities may be written as follows:

$$\begin{aligned} I_l &= A' [1 - B' Z^i(\xi)] / d_l, \\ I_h &= A' [1 - B' Z^i(\xi)] / d_h. \end{aligned} \quad (5)$$

The parameters A' and B' describe the loss and gain in the medium; N_0 is the excitation parameter; $Z(\xi)$ is the plasma dispersion function; I_1 and I_2 are the velocity integrals¹ ($\text{Re} I_2$ gives the usual Lorentzian in the Doppler-limit approximation) whereas S , S_1 , S_2 , and S_3 represent the sums¹²

$$\begin{aligned} S &= \sum_m |\mu_{am} \mu_{b, m+1}|^2, & S_2 &= \sum_m |\mu_{am} \mu_{b, m+1}|^2 |\mu_{b, m+1} \mu_{a, m+2}|^2, \\ S_1 &= \sum_m |\mu_{am} \mu_{b, m+1}|^4, & S_3 &= \sum_m |\mu_{am} \mu_{b, m+1}|^2 |\mu_{am} \mu_{b, m-1}|^2. \end{aligned}$$

For the 3.39- μm line in particular ($J_b = 1$, $J_a = 2$) $S_1 \sim 46$, $S_2 \sim 21$, and $S_3 \sim 1$. The $\Gamma_{a,b}'(0)$ and $\Gamma_{a,b}'(2)$ describe the relaxation rates of the level populations and of the Zeeman coherences. By equating in the weak-pressure approximation³ the different relaxation rates $\Gamma_{a,b}'$ for this line,¹³ it is seen that, for the same excitation, the ratio of the denominators of (5) becomes at line center

$$d_h/d_l = (2S_1 + S_2 + S_3)/2(S_1 + S_2 + S_3) \approx 0.84.$$

More important is the fact that the I_2 integral coefficients describing the Lamb dips are in a ratio

$$(S_1 + S_2 + S_3)/(S_2 + S_3) \approx 3.$$

Hence the Lamb dip should be enhanced by a factor of 3 by changing the helicoidal polarization into a linear one. Comparison of experimental data with theory can be done directly using expressions (3) and (4). However, in order to compare our results with other works, we first utilize the phenomenological formula proposed for a linearly polarized wave by Szöke and Javan² and modified by Cordover

and Bonczyk,² i.e.,

$$I(X) = A[1 - B \exp(X^2)] \left[\left(1 - \frac{2C}{\sqrt{\pi}}\right) + D \left(1 + \frac{2C}{\sqrt{\pi}}\right) \frac{C^2}{C^2 + (X - E)^2} \right]^{-1}, \quad (6)$$

where D appears as an enhancement coefficient of the Lamb dip. The theoretical curves corresponding to this formula have been reported in Figs. 2 and 3 with the following parameters: $B = 0.588$, $C = 0.165$, $E = 0.03$; A is an amplitude parameter; $D_l = 0.15$ in the case of a linear wave; and $D_h = 0.05$ in the case of the helicoidal wave. We see that the enhancement coefficient D_l in the linear-wave case is three times greater than the D_h for the helicoidal wave in agreement with our previous calculations. We find also as ratio at line center of the denominators of the phenomenological formula $d_h/d_l \approx 0.87$, which is very close to that predicted theoretically. The usual linearly polarized Lamb dip at $3.39 \mu\text{m}$ therefore appears as partially anisotropic. Very good agreement with experimental points for both polarizations is observed. The B parameter of expression (6) has been experimentally evaluated to $B = (\text{losses})/(\text{unsaturated gain}) = 0.60$. Equations (3) and (4) lead to identical theoretical curves directly derived from I_1 and I_2 integrals.¹⁴

We have therefore obtained, with the helicoidal wave, a simple decomposition of the Lamb dip into two experimentally separable contributions. In agreement with the theoretical analysis the nature and enhancement of the Lamb dip depends on the saturating field polarization and on the level degeneracies. We note also that to the three sums S_1 , S_2 , and S_3 which characterize the laser line correspond to the three possible Lamb-dip profiles; indeed, in addition to the two preceding profiles, one can consider that obtained with a circular field polarization (in this case only S_1 occurs in the intensity denominator). This can be extended to the absorption case outside the resonator, giving a new method of investigation of J levels (kinetic momenta, etc.). Further information on the asymmetry seen on the Lamb dip at $3.39 \mu\text{m}$ and also observed by Bennett¹⁵ might be obtained with use of our analysis.

The authors wish to thank Tran Chanh Truc for his help in carrying out some of the calculations.

¹W. E. Lamb, Jr., Phys. Rev. **134**, A1429 (1964); M. Sargent, III, M. O. Scully, and W. E. Lamb, Jr., *Laser Physics* (Addison-Wesley, Reading, Mass., 1974).

²A. Szöke and A. Javan, Phys. Rev. **145**, 137 (1966); R. H. Cordover and P. A. Bonczyk, Phys. Rev. **188**, 696 (1969).

³M. Dumont, thesis, Université de Paris, 1970 (unpublished); I. M. Beterov, Yu Matyugin, and V. P. Chebotayev, Opt. Spectrosc. **28**, 191 (1970).

⁴W. R. Bennett, Jr., Phys. Rev. **126**, 580 (1962), and Appl. Opt., Suppl. **1**, No. 1, 24 (1962), and in *Proceedings of the Third International Conference on Quantum Electronics, Paris, 1963*, edited by P. Grivet and N. B. Bloembergen (Columbia Univ. Press, New York, 1961), Vol. 9, p. 441.

⁵A. Le Floch, R. Le Naour, and C. Stephan, Opt. Commun. **20**, 42 (1977).

⁶R. L. Fork and M. Sargent, III, Phys. Rev. **139**, A617 (1965).

⁷A. Le Floch and R. Le Naour, Phys. Rev. A **4**, 290 (1971).

⁸V. Evtuhov and A. E. Siegman, Appl. Opt. **4**, 142 (1965).

⁹A. Kastler, C. R. Acad. Sci., Ser. B **271**, 999 (1970).

¹⁰A. Le Floch and G. Stephan, C. R. Acad. Sci., Ser. B **277**, 265 (1973).

¹¹G. Stephan, R. Le Naour, and A. Le Floch, Phys. Rev. A (to be published).

¹²C. V. Heer and R. D. Graft, Phys. Rev. **140**, A1088 (1965).

¹³R. T. Menzies, U. S. Air Force Office of Scientific Research Report No. 11-AF-AFOSR 68-1492, 1965 (unpublished).

¹⁴M. Sargent, III, and M. O. Scully, in *Laser Handbook*, edited by F. T. Arecchi and E. D. Schulz-Dubois (North-Holland, Amsterdam, 1972), Vol. 1, p. 81.

¹⁵W. R. Bennett, Jr., S. F. Jacobs, J. T. LaTourrette, and R. Rabinowitz, Appl. Phys. Lett. **5**, 56 (1964).